Electrochimica Acta 115 (2014) 146–154

Contents lists available at ScienceDirect

Electrochimica Acta

journal homepage: www.elsevier.com/locate/electacta

Electro and photoelectrochemical reduction of carbon dioxide on multimetallic porphyrins/polyoxotungstate modified electrodes

Macarena García[a], M. Jesús Aguirre[b], Gabriele Canzi[c], Clifford P. Kubiak[c], Macarena Ohlbaum[d], Mauricio Isaacs[d,*]

[a] Facultad de Ciencias, Departamento de Química, Universidad de Chile, Las Palmeras #3425, casilla 653, Ñuñoa, Santiago, Chile
[b] Facultad de Química y Biología, Departamento de Química de los Materiales, Universidad de Santiago de Chile, Av. Bernardo O'Higgins 3363, Estación Central, Casilla 40- correo 33, Santiago, Chile
[c] Department of Chemistry and Biochemistry, University of California San Diego, 9500 Gilman Drive MC 0358, La Jolla, CA 92093, USA
[d] Departamento de Química Inorgánica, Facultad de Química, Pontificia Universidad Católica de Chile, Av. Vicuña Mackenna #4860, Macul, Santiago, Chile

ARTICLE INFO

Article history:
Received 29 April 2013
Received in revised form
23 September 2013
Accepted 20 October 2013
Available online 1 November 2013

Keywords:
Carbon dioxide
Porphyrin
Polyoxometalate
Modified electrode
Electrocatalysis
Photoelectrocatalysis

ABSTRACT

Electrochemical and photoelectrochemical reduction of carbon dioxide was studied in aqueous solution, using an ITO/multilayer modified electrode. The multilayer formation was carried out by the Layer-by-Layer method (LBL), using a μ-(meso-5,10,15,20-tetra(pirydil)porphyrin)tetrakis {bis(bipyridine)chloride ruthenium(II)} coordinated with Mn(III), Zn(II) and Ni(II) in its central cavity and an anionic polyoxotungstate $[SiW_{12}O_{40}]^{4-}$. The multilayer formation was corroborated by electrochemical methods and UV–visible spectroscopy. For this study, 3 multilayers were formed on the ITO surface. Carbon dioxide reduction was studied by linear sweep voltammetry at pseudo stationary state ($5\,mV\,s^{-1}$) in a 0.1 M $NaClO_4$, CO_2 saturated solution. Photoelectrochemical reduction of carbon dioxide was studied in the same conditions described above under light irradiation at 440 nm. In dark conditions, an enhancement in current is detected at −0.75 V indicating carbon dioxide reduction. Under light irradiation the reduction process shifts to −0.60 V. Chemical analysis after controlled potential electrolysis shows that in dark conditions, formic acid, carbon monoxide and methanol are the reduction products. Under light irradiation there is a change in the product distribution and for some metals; formaldehyde can be detected, evidencing a change in the reduction mechanism. These results support the fact that $[MTRP]^{n+}/[SiW_{12}O_{40}]^{4-}$ multilayer modified electrodes act as electrocatalysts for carbon dioxide reduction and that this activity is enhanced by a combination of light and potential where light produces excited states sites on the multilayer, that are more reactive toward carbon dioxide reduction.

1. Introduction

The reduction of global CO_2 emissions is currently an issue of major concern [1,2] due to its increase in the atmospheric concentration, caused by the dependence of human population on fossil fuels for energy sources, which is considered the major cause of the greenhouse effect [3–5]. This has stimulated the development of electrochemical and photoelectrochemical systems able to produce useful organic chemicals by reducing CO_2 gas [6].

The electrochemical reduction of CO_2 usually requires a high overpotential of approximately −2 V vs NHE [7,8] for a one electron process. This potential can be lowered, by performing a two electron or proton coupled multi-electron CO_2 reduction [8,9], with the necessary CO_2 activation performed with the use of a catalyst. This suggests that a multi-electron redox system is necessary for constructing a practical electrocatalytic system for CO_2 reduction.

For the study of this reaction, a wide range of electrodes has been used: metallic cathodes such as Cu, Hg, Au, Ag, Ni, Pt [10–13] and semiconductors such p-CdTe, p-InP, p-GaAs [14–16]. The use of carbon electrodes, have also been studied, but in this case, a high overpotential is required and depending on the solvent, hydrogen evolution can compete as a secondary reaction [17]. This problem has been solved, using different kinds of catalyst such as transition metal complexes which can act as an electronic mediator and exhibit electro and photoelectrocatalytic activity toward CO_2 reduction, in homogeneous media and confined on electrodes [9,17–24].

Macrocyclic metal complexes, such porphyrins and pthalocyanines have been widely studied as electrocatalysts in solution and forming parts of modified electrodes [21,25,26]. Results show that the efficiency and selectivity depend on different factors, for example the reaction media, applied potential, and microenvironment.

* Corresponding author. Tel.: +56 2 3544393.
E-mail address: misaacs@uc.cl (M. Isaacs).

0013-4686/$ – see front matter © 2013 Elsevier Ltd. All rights reserved.
http://dx.doi.org/10.1016/j.electacta.2013.10.142

Araki and coworkers synthesized a tetraruthenated porphyrin, consisting on a free base μ-{meso-5,10,15,20-tetra(pyridyl)porphyrin}tetrakis{bis(bipyridyne)chloride ruthenium (II)}$(PF_6)_4$ (TRP) and the metal complexes derivates (Co(II), Ni(II), Zn(II)) [27] These types of supramolecular complexes have been used in electrocatalytic studies for sulfite reduction, nitrite oxidation and reduction, oxygen reduction and carbon dioxide reduction in solution [28–32]. Its capacity to act as an efficient electrocatalyst is mainly due to the combination of the catalytic and redox properties of porphyrins and the redox and photochemical properties of ruthenium polypyridyl complexes, which improve the electron transfer.

On the other hand, photoelectrochemical reduction of CO_2 has been studied with mixed systems such as $[Ru(bipy)_3]^{2+}$ and $[Ru(bipy)_2(CO)_2]^{+}$ [7,33]. In this system, $[Ru(bipy)_3]^{2+}$ acts as a photosensitizer and $[Ru(bipy)_2(CO)_2]^{+}$ as a catalyst in the presence of a reductant such a NAD(P)H model compound. [Co(tetraaza-macrocycles)]$^{2+}$ [34] and [Ni(cyclam)]$^{2+}$ [35,36] have also been used as catalysts in the presence of a photosensitizer obtaining CO as a major product, however, for this type of system, the efficiency of CO_2 reduction has several drawbacks, since hydrogen evolution from hydride complexes forms in the catalytic cycle. Different types of semiconductors have been used for CO_2 photoelectrochemical reduction [14–16,5,37] obtaining different reduction products such as methane, methanol, ethanol, formaldehyde and formic acid [14–16,5,37].

Polyoxometalates (POMs) are a group of early transition metal–oxygen clusters. Their versatile nature in terms of size, redox chemistry, structure, charge distribution and photochemistry means that polyoxometalate chemistry is arguably one of the many areas in inorganic chemistry that is developing most rapidly today [38]. Thin films of POMs in combination with water soluble cations [39], nanoparticles [40–42] and polymers [43,44] have been previously reported. In the last decade POMs have been recognized as important building blocks for highly efficient photocatalyst and photoelectrochemical devices when combined with semiconductors and organic/inorganic molecules [45]. It has been reported that in acid media a modified electrode with heteropoly and isopolyoxometalates shows high activity towards the hydrogen evolution reaction (HER) and molecular oxygen reduction [46], which has also been studied for nitrite, bromate and iodate reduction [47–49]. Cationic porphyrins combined with POMs give rise to an organic-inorganic film with very interesting electrocatalytic behavior for molecular oxygen reduction generating hydrogen peroxide as the reduction product and for hydrogen evolution in the range of −0.4/−0.5 V [46,50–52].

To the best of our knowledge there are no studies of carbon dioxide reduction and photoelectroreduction on multimetallic porphyrins/POMs films. The present work describes carbon dioxide reduction with an ITO/multilayer modified electrode. The multilayer was generated by a combination of cationic metal center Mn(III), Zn(II) and Ni(II) μ-{meso-5, 10, 15, 20-tetra (pyridyl) porphyrin} tetrakis {bis(bipyridine)chloride ruthenium(II)} ($[Mn(III)TRP]^{5+}$, $[Zn(II)TRP]^{4+}$ and $[Ni(II)TRP]^{4+}$, respectively) and an anionic polyoxotungtate $[SiW_{12}O_{40}]^{4-}$ using a *layer-by-layer* method. Electroreduction and photoelectroreduction of carbon dioxide was studied in aqueous solution, by linear sweep voltammetry in the range between 0 and −0.9 V and controlled potential electrolysis.

Reduction products detection was carried out by colorimetric and chromatographic methods. Stability of these multilayer films was evaluated, before and after potential controlled electrolysis experiments.

These studies confirm the capability of these multilayer modified electrodes to act as electro and photoelectrocatalyst favoring single or multiple charge transfer process.

2. Experimental

2.1. Chemical reagents

All chemical reagents were of analytical grade. Polyoxotungstate anion $[SiW_{12}O_{40}]^{4-}$ and ammonium hexafluorophosphate were purchased from Fluka. Mn(III) acetate, Zn(II) acetate, Ni(II) acetate, 5,10,15,20-tetra pyridyl-21*H*, 23*H*-porphine, sodium perchlorate and 2,2-dipyridyl were purchased from Sigma-Aldrich. Lithium chloride was purchased from Fisher Scientific. Ruthenium(III) chloride trihydrate was purchased from Pressure Chemical Co.

N,*N*-dimethylformamide (DMF), ethanol, methanol, acetone, glacial acetic acid and neutral alumina were purchased from Merck.

The synthesis of the precursor complex *cis*-dichloro (2,2-bipyridine) ruthenium(II) dihydrate was carried out based on a procedure previously described in the literature [53]. Supramolecular complexes $[Mn(III)TRP]^{5+}$, $[Zn(II)TRP]^{4+}$ and $[Ni(II)TRP]^{4+}$ were prepared by a method described by Araki et al. [30,32,54–56]. The purity of these compounds was checked by optical absorption spectroscopy, elemental analysis and cyclic voltammetry.

2.2. Procedures

Electrochemical experiments were carried out in a CH Instruments model 620B electrochemical workstation using a three compartment Pyrex glass cell. An ITO electrode (Delta Technologies, USA) was used as the working electrode with Ag/AgCl (CH Instruments, TX, USA) as the reference electrode, and Pt wire as the counter.

All potentials values informed in this work are quoted against Ag/AgCl reference electrode. Photoelectrochemical experiments were carried out using a three compartment cell with a quartz window irradiated with light provided by a 500 W Xenon-Mercury lamp system (Oriel Co) coupled to a monochromator (Jarrell Ash, Czerny-turner). Controlled potential electrolysis experiments were carried out on a BASI POWER MODULE PWR-3 potentiostat. The experiments were performed in a gastight H type cell. UV–Visible data were recorded on a Shimadzu Multispec 1501 spectrophotometer. Gas chromatography measurements were carried out using a DANI Master GC with a FID and a TCD detector. The columns used were a Supelcowax 10 (30 m × 0.32 mm × 0.25 μm film thickness) and a Supelco mol sieve 5A° (30 m × 0.53 mm).

2.2.1. Preparation of the $[MTRP]^{n+}/[SiW_{12}O_{40}]^{4-}$ multilayer film

The ITO electrode was cleaned with methanol for one hour, and subsequently rinsed with deionized water for an additional hour.

Multilayer formation was carried out by a previously reported method [57]. A cleaned ITO electrode was dipped into a 0.5 mM methanolic solution of Ni(II), Zn(II) or Mn(III) porphyrin for 4 min. The electrode was rinsed with deionized water to avoid surface excess. The layer modified ITO electrode was dipped into a 0.5 mM water solution of $[SiW_{12}O_{40}]^{4-}$ for 4 min. The bilayer modified ITO electrode was rinsed and dried. The procedure was repeated three times, obtaining a multilayer $[MTRP]^{n+}/[SiW_{12}O_{40}]^{4-}$ modified electrode.

The multilayer formation was monitored by cyclic voltammetry and UV–Vis spectroscopy.

The stability of multilayer modified electrode was evaluated in a 0.1 M $NaClO_4$ solution. The potential electrode was swept during 50 continuous cycles between −0.9 V and 1.0 V

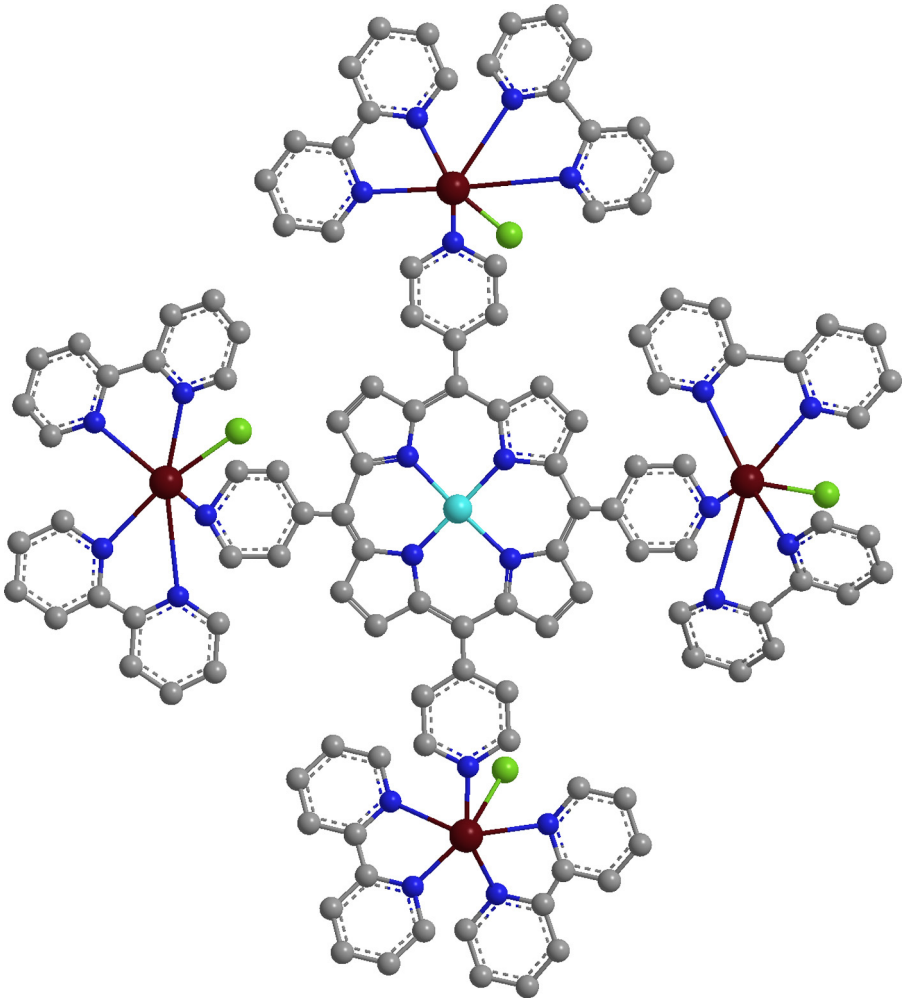

Fig. 1. Structural representation of M(III), Ni(II) and Zn(II) μ-(meso-5,10,15,20 tetra(pirydil)porphyrin)tetrakis {bis(bipyridine)chloride ruthenium(II)}.

for $[Zn(II)TRP]^{4+}/[SiW_{12}O_{40}]^{4-}$ and $[Mn(III)TRP]^{5+}/[SiW_{12}O_{40}]^{4-}$ multilayer modified electrode and between −0.9 V and 1.2 V for $[Ni(II)TRP]^{4+}/[SiW_{12}O_{40}]^{4-}$ multilayer modified electrode.

2.2.2. Electrochemical reduction of carbon dioxide

The electroreduction process of carbon dioxide was studied by linear sweep voltammetry (LSV) with $[MTRP]^{n+}/[SiW_{12}O_{40}]^{4-}$ multilayer modified electrode, in a 0.1 M $NaClO_4$ aqueous solution saturated with CO_2, between −0.1 V and −0.9 V at 5 mV s^{-1}.

2.2.3. Photoelectrochemical reduction of carbon dioxide

Photoelectrochemical reduction experiments were studied by LSV in a 0.1 M $NaClO_4$ aqueous solution saturated with CO_2, between −0.1 V and −0.9 V at 5 mV s^{-1}. For this study the electrode was 5 cm from the lamp where the light intensity was 20 mW cm^{-2}.

2.2.4. Controlled potential electrolysis

Controlled potential electrolysis experiments were carried out using a three multilayer $[MTRP]^{n+}/[SiW_{12}O_{40}]^{4-}$ modified electrode. In dark conditions the experiment was carried out for 6 h at −0.8 V. Under light irradiation the time of electrolysis was 3 h and the potential was set at −0.65 V.

The analysis of aqueous products (formic acid and formaldehyde) were carried out using previously reported methods [19,58]. Gaseous products were determined by gas chromatography.

3. Results and discussion

3.1. Multilayer $[MTRP]^{n+}/[SiW_{12}O_{40}]^{4-}$

Fig. 1 presents the structure of a tetraruthenated porphyrin consisting in a free (or metallated with M = Mn(II), Zn(II) and Ni(II)) μ-(meso-5,10,15,20-tetra(pirydil)porphyrin)tetrakis coordinated to four groups {bis(bipyridine)chloride ruthenium(II)}[57].

The electronic spectra of $[Mn(III)TRP]^{5+}$, $[Zn(II)TRP]^{4+}$ and $[Ni(II)TRP]^{4+}$ are similar. The characteristic Soret ($\pi \rightarrow \pi^*$) and Q ($\pi \rightarrow \pi^*$) band appears and the energy of these transitions depends of the electronic environment caused by the metal center coordinated to the porphyrin. The Soret band appear at 464, 426 and 410 nm for $[Mn(III)TRP]^{5+}$, $[Zn(II)TRP]^{4+}$ and $[Ni(II)TRP]^{4+}$, respectively. Q bands appears at 580 and 630 nm for the $[Mn(III)TRP]^{5+}$, at 560 and 603 nm for $[Zn(II)TRP]^{4+}$ and in the case of $[Ni(II)TRP]^{4+}$ only one Q band is observed at 530 nm. The three metalloporphyrins exhibit a strong band at 292 nm which correspond to a $\pi \rightarrow \pi^*$ transition of the $\{Ru(bipy)_2Cl\}^+$ ligand [30,59], a band at 355 nm, which is assigned as a metal-to-ligand transfer band (MLCT2) ($Ru^{II}(d\pi) \rightarrow$ bipy (π_2^*)) [30,59] and another band at 490 nm, which is also assigned as a MLCT ($Ru^{II}(d\pi) \rightarrow$ bipy (π_1^*)) (overlapped with the Soret band) [30,59]. The polyoxotungstate anion has only one transition at 260 nm corresponding to a W → O charge transfer band [50].

When the multilayer formation was monitored, for the $[Mn(III)TRP]^{5+}/[SiW_{12}O_{40}]^{4-}$ and $[Zn(II)TRP]^{4+}/[SiW_{12}O_{40}]^{4-}$, the

Table 1
Redox processes of porphyrin complexes and polyoxotungstate.

Compounds	$P^{(2-/-)}$	$P^{(-/0)}$	$M^{(3+/2+)}$	$Ru^{(3+/2+)}$	
$[Mn(III)TRP^{5+}]$	−1.1	−0.99	−0.06	0.85	
$[Zn(II)TRP^{4+}]$	–	−1.025	–	0.808	
$[Ni(II)TRP]^{5+}$	−1.09	−1.01	0.27	0.75	
	$H_2PM^{8-/7-}$	$H_2PM^{7-/6-}$	H_2PM^{6-}/PM^{6-}	$PM^{(6-/5-)}$	$PM^{(5-/4-)}$
$[SiW_{12}O_{40}{}^{4-}]$	−0.9*	−0.8*	−0.55	−0.45	−0.2

* Redox processes associated with chemical reactions.

spectra display the $[MTRP]^{n+}$ transitions describes above, and in both cases, the absorbance of all transitions increase linearly with the number of multilayers deposited on the ITO surface demonstrating an increase of the chromophore concentration on the ITO surface [57]. It is important to mention that with each multilayer, the Soret band presents a slight blue shift (2 nm for the $[Mn(III)TRP]^{5+}/[SiW_{12}O_{40}]^{4-}$ multilayer and 5 nm for the $[Zn(II)TRP]^{4+}/[SiW_{12}O_{40}]^{4-}$ multilayer [57]) due to aggregation that can occur between layers. This effect is more prevalent with the $[Ni(II)TRP]^{4+}/[SiW_{12}O_{40}]^{4-}$ multilayer assembly. In this case, the multilayer spectra presents four transitions (see supporting information), resembling spectra in solution of $[Ni(II)TRP]^{4+}$. However, a widening and a blue shift in all bands is apparent due to the high aggregation of the porphyrin due to strong π–π interactions between the porphyrins skeleton [59–62]. It is important to mention that the absorbance value of all bands, increase linearly with the number of multilayer deposited on the surface.

Cyclic voltammetry experiments of $[Mn(III)TRP]^{5+}$, $[Zn(II)TRP]^{4+}$ and $[Ni(II)TRP]^{4+}$ were recorded at 1 mM macrocyclic solution and 0.1 M TBPA as supporting electrolyte, in DMF. For $[SiW_{12}O_{40}]^{4-}$, the experiment was performed in a 1 mM polyoxotungstate solution in a 0.5 M H_2SO_4 solution (supporting electrolyte). The obtained data are summarized in Table 1, all the redox processes were assigned according to literature [30,47,59,63,64]. As it can be seen, polyoxotungstate anion present five redox processes in acid media. Three of these processes depend on the pH of the solution. Considering that this anion presents an acid/base equilibrium, its stability in the working medium (pH = 5.7) was studied evaluating the UV–Visible spectrum of the compound after 24 and 48 h. No further changes were detected in the UV–Visible spectrum, corroborating the stability of this anion in the working media.

The multilayer formation was followed by cyclic voltammetry. After each multilayer deposition, a voltammogram was recorded, in a 0.1 M $NaClO_4$ solution between −0.9 V and 1.0 V vs Ag/AgCl for the $[Mn(III)TRP]^{5+}$ and $[Zn(II)TRP]^{4+}$ multilayers, and between −0.9 V and 1.1 V vs Ag/AgCl for the $[Ni(II)TRP]^{4+}/[SiW_{12}O_{40}]^{4-}$ multilayer. All the experiments were recorded at 100 mV s^{-1}. Fig. 2a displays the voltammetric response of an ITO electrode after the deposition of 1, 2 and 3 $[Ni(II)TRP]^{4+}/[SiW_{12}O_{40}]^{4-}$ multilayers. At positive potentials the voltammogram shows a reversible wave corresponding to the $Ru^{III/II}$ process [28,57]. At negative potentials, the voltammogram presents a single wave at −0.85 V which corresponds to a reduction process of the multilayer film related to porphyrin redox processes (see inset in Fig. 2a). This reduced multilayer film is reoxidized at 0.45 V vs Ag/AgCl where the appearance of an oxidative peak is noticeable (see supporting information). Results show (Fig. 2), that with the increase of each multilayer, the charge of the Ru^{III}/Ru^{II} process increases linearly, indicating an increment of the electroactive material on the electrode surface. With the increased number of bilayers, this process becomes more irreversible indicating that the electron transfer becomes slower [57].

As shown in Fig. 2b strong correlation is found between the value of the absorbance at the Soret band and the charge of the cathodic and anodic Ru^{III}/Ru^{II} process with the number of multilayers.

For the $[Mn(III)TRP]^{5+}/[SiW_{12}O_{40}]^{4-}$ and $[Zn(II)TRP]^{4+}/[SiW_{12}O_{40}]^{4-}$ multilayer modified electrode, the voltammogram shows a similar electrochemical response, showing at positive potentials, the $Ru^{III/II}$ process and at −0.7 V vs Ag/AgCl a process which correspond to the multilayer reduction as it was reported previously [57].

The electrochemical stability of this modified electrodes, was evaluated by studying the variation of the charge under the voltammetric anodic and cathodic peak of the Ru^{III}/Ru^{II} process over 50 continuous voltammetric cycles in a 0.1 M $NaClO_4$ solution at 100 mV s^{-1}. Under these experimental conditions, the three

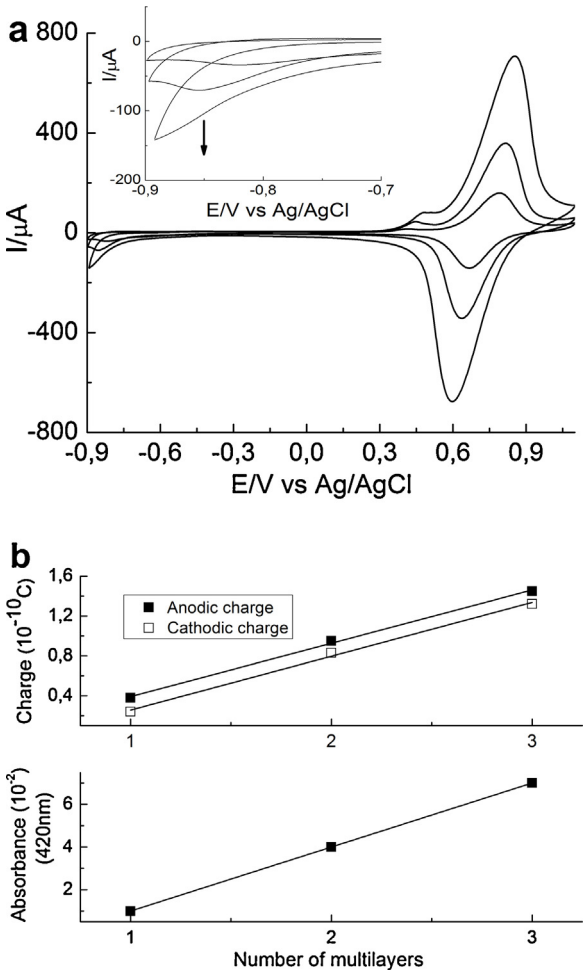

Fig. 2. (a) Cyclic voltammetry of a 1, 2 and 3 $[Ni(II)TRP]^{4+}/[SiW_{12}O_{40}]^{4-}$ multilayers modified electrode. 0.1 M $NaClO_4$ solution. Scan rate 100 mV s^{-1}. (b) Relation between the absorbance at the Soret band and the charge of the cathodic and anodic Ru^{III}/Ru^{II} process with the number of multilayers on the ITO surface.

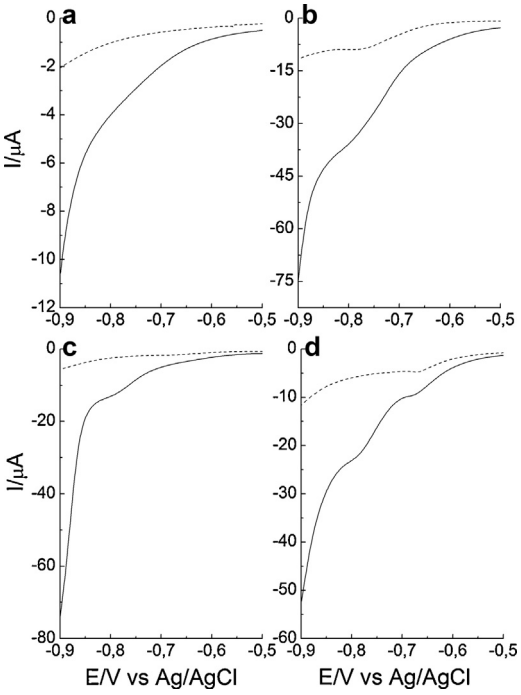

Fig. 3. Linear sweep voltammogram of (a) bare ITO electrode (b) $[Mn(III)TRP]^{5+}/[SiW_{12}O_{40}]^{4-}$ multilayer modified electrode (c) $[Zn(III)TRP]^{4+}/[SiW_{12}O_{40}]^{4-}$ modified electrode and (d) $[Ni(II)TRP]^{4+}/[SiW_{12}O_{40}]^{4-}$ modified electrode in presence (solid line) and absence (dash line) of CO_2. 0.1 M $NaClO_4$ solution saturated with CO_2 at 5 mV s^{-1}. Potentials are versus Ag/AgCl.

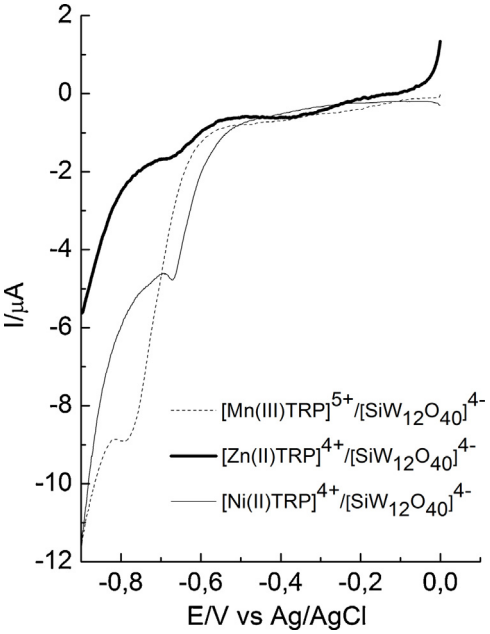

Fig. 4. Polarization curves of a 3[MTRP]/$[SiW_{12}O_{40}]^{4-}$ multilayer modified electrode under N_2 atmosphere. 0.1 M $NaClO_4$ solution, scan rate 5 mV s^{-1}.

modified electrodes were stable showing no significant decrease of the charge (less than 5%).

3.2. Electrochemical reduction of CO_2

Fig. 3 displays *I/E* curves of $[MTRP]^{n+}/[SiW_{12}O_{40}]^{4-}$ multilayer modified electrodes in pseudo steady state conditions recorded at 5 mV s^{-1} in presence and absence of CO_2.

As it can be seen, the three modified electrodes (Fig. 3b–d) present electrocatalytic activity toward the electrochemical reduction of carbon dioxide. In all cases, an increase in the cathodic current can be observed.

The bare ITO electrode (Fig. 3a), shows an increase in the cathodic current around −0.6 V vs Ag/AgCl, however this current is less than the multilayers modified electrodes.

The shape of the voltammogram under inert atmosphere, presents different patterns for each electrode (see Fig. 4). $[Mn(III)TRP]^{5+}/[SiW_{12}O_{40}]^{4-}$ modified electrodes show a single process at −0.8 V vs Ag/AgCl, $[Zn(II)TRP]^{4+}/[SiW_{12}O_{40}]^{4-}$ show two reduction process at −0.37 V and −0.67 V vs Ag/AgCl and $[Ni(II)TRP]^{4+}/[SiW_{12}O_{40}]^{4-}$ show one reduction processes at −0.67 V vs Ag/AgCl. These processes correspond to the multilayer reduction. Carbon dioxide reduction at $[Mn(III)TRP]^{5+}/[SiW_{12}O_{40}]^{4-}$, $[Zn(II)TRP]^{4+}/[SiW_{12}O_{40}]^{4-}$ and $[Ni(II)TRP]^{5+}/[SiW_{12}O_{40}]^{4-}$ multilayer modified electrode takes place at −0.6 V, −0.65 V and −0.6 V vs Ag/AgCl (onset potential), respectively. In all cases, the multilayer reduction process (described before) is enhanced by the presence of carbon dioxide and for the $[Ni(II)TRP]^{4+}/[SiW_{12}O_{40}]^{4-}$ multilayer a new peak appears at −0.75 V vs Ag/AgCl which corresponds to the reduction of an electroactive species that were not detected under inert atmosphere, which is active toward carbon dioxide reduction. It could also be an adsorbed product from carbon dioxide reduction assisted by a ligand.

Results suggest that the reduced species in the multilayers are the active moiety in carbon dioxide reduction.

Comparing the cathodic current observed for the three modified electrodes in presence of carbon dioxide at the same potential (−0.8 V vs Ag/AgCl) it is clear that the $[Mn(III)TRP]^{5+}/[SiW_{12}O_{40}]^{4-}$ multilayer modified electrode presents the highest current response with a value of −36.0 μA which is around nine times higher with respect to the bare ITO electrode. The $[Zn(II)TRP]^{4+}/[SiW_{12}O_{40}]^{4-}$ multilayer modified electrode shows a current increment of approximately three times and $[Ni(II)TRP]^{4+}/[SiW_{12}O_{40}]^{4-}$ presents a current increment of around six times the bare ITO electrode. The current increase of the three modified electrodes in comparison with the bare ITO electrode confirms the catalytic activity of the multilayers arrangements adsorbed onto the ITO surface. It can be concluded that the current value reached for carbon dioxide reduction presents the following trends: $[Mn(III)TRP]^{5+}/[SiW_{12}O_{40}]^{4-}$ multilayer > $[Ni(II)TRP]^{4+}/[SiW_{12}O_{40}]^{4-}$ multilayer > $[Zn(II)TRP]^{4+}/[SiW_{12}O_{40}]^{4-}$ multilayer.

3.3. Reduction products—Controlled potential electrolysis

The reduction products in the electrochemical reduction of carbon dioxide, at $[MTRP]^{n+}/[SiW_{12}O_{40}]^{4-}$ multilayer modified electrodes were determined after controlled potential electrolysis experiments. Carbon monoxide, formic acid and methanol were detected as the reduction products, corresponding to a transfer of two and six electrons as it can be seen in Eqs. (1)–(3).

$$CO_2 + 2H^+ + 2e^- \rightarrow CO + 2H0 \quad (1)$$

$$CO_2 + 2H^+ + 2e^- \rightarrow HCOOH \quad (2)$$

$$CO_2 + 6H^+ + 6e^- \rightarrow CH_3OH + H_2O \quad (3)$$

No other products were detected by the analytical methods performed in this work.

The results obtained for the electrolysis experiments, carried out for 6 h using a $[Mn(III)TRP]^{5+}/[SiW_{12}O_{40}]^{4-}$, a

Table 2
potential controlled electrolysis results; after 6 h, in a 0.1 M $NaClO_4$ solution saturated with CO_2, at −0.8 V.

Multilayer	Formic acid (mM)	TOF (s^{-1})	TON	Methanol (mM)	TOF (s^{-1})	TON	CO (mM)	TOF (s^{-1})	TON
$[Mn(III)TRP]^{5+}/[SiW_{12}O_{40}]^{4-}$	1.5×10^{-1}	4.8×10^{-1}	1.06×10^{4}	6.99×10^{-3}	2.3×10^{-2}	5.0×10^{2}	–	–	–
$[Zn(II)TRP]^{4+}/[SiW_{12}O_{40}]^{4-}$	1.8×10^{-3}	3.7×10^{-3}	8.3	3.8	8.2	1.76×10^{5}	–	–	–
$[Ni(II)TRP]^{5+}/[SiW_{12}O_{40}]^{4-}$	2.6×10^{-2}	8.3×10^{-2}	1.8×10^{3}	–	–	–	3.85×10^{-2}	2.4×10^{-1}	3.85×10^{3}
Bare ITO	9.3×10^{-4}	–	–	1.35×10^{-2}	–	–	–	–	–

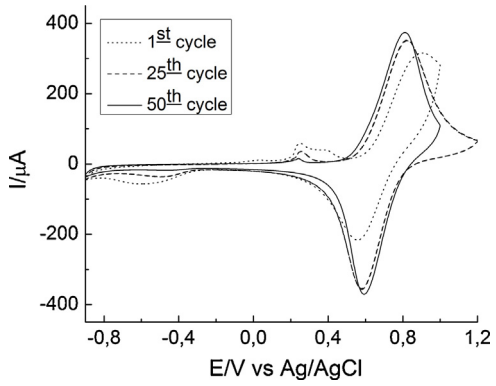

Fig. 5. 1st, 25th and 50th voltammetric cycle of an $[Mn(III)TRP]^{5+}/[SiW_{12}O_{40}]^{4-}$ multilayer modified electrode after potential controlled electrolysis experiments. 0.1 M $NaClO_4$ solution, scan rate 100 mV s^{-1}.

$[Zn(II)TRP]^{4+}/[SiW_{12}O_{40}]^{4-}$ and a $[Ni(II)TRP]^{4+}/[SiW_{12}O_{40}]^{4-}$ multilayer modified electrode, are tabulated in Table 2.

At the working potential, higher concentrations of formic acid are obtained with $[Mn(III)TRP]^{5+}/[SiW_{12}O_{40}]^{4-}$ multilayer modified electrodes, and give rise to the following trend: $[Mn(III)TRP]^{5+}/[SiW_{12}O_{40}]^{4-}$ multilayer > $[Ni(II)TRP]^{4+}/[SiW_{12}O_{40}]^{4-}$ multilayer > $[Zn(II)TRP]^{4+}/[SiW_{12}O_{40}]^{4-}$ multilayer > bare ITO. On the other hand, for methanol production the trends change, with the $[Zn(II)TRP]^{4+}/[SiW_{12}O_{40}]^{4-}$ multilayer modified electrode showing the major activity, followed by the $[Mn(III)TRP]^{5+}/[SiW_{12}O_{40}]^{4-}$ multilayer modified electrode. For the $[Ni(II)TRP]^{4+}/[SiW_{12}O_{40}]^{4-}$ multilayer modified electrode no activity toward methanol production is observed, but carbon monoxide was detected as a reduction product.

TOF (turn over frequency) [65] and TON (turn over number) [66,67] values, are also presented in Table 2. TON is described as the number of moles of product that a catalyst can produce before becoming inactivated and it was calculated as: moles of product formed per mol of catalyst. TOF values were calculated as the turnover number per unit of time (s) and geometric area of the electrode (cm^2). Both parameters are related with the real catalytic activity of each multilayer film. An ideal catalyst will present high TON and TOF values. As it can be seen, $[Mn(III)TRP]^{5+}/[SiW_{12}O_{40}]^{4-}$ multilayer modified electrode shows the biggest TOF and TON values for formic acid production and $[Zn(II)TRP]^{4+}/[SiW_{12}O_{40}]^{4-}$ multilayer modified electrode exhibit the biggest TOF and TON values for methanol production.

The electrochemical activity of the $[MTRP]^{n+}/[SiW_{12}O_{40}]^{4-}$ multilayer modified electrode, after 6 h of potential controlled electrolysis, was evaluated by studying the variation of the voltammogram shape and evaluating the charge under the voltammetric anodic and cathodic peak of the Ru^{III}/Ru^{II} process in a 0.1 M $NaClO_4$ solution. Fig. 5 shows the voltammetric response of an $[Mn(III)TRP]^{5+}/[SiW_{12}O_{40}]^{4-}$ multilayer modified electrode after potential controlled electrolysis experiments. The first cycle presents a different voltammetric response, where the Ru^{III}/Ru^{II} process appears as a more irreversible couple instead of a reversible couple. At negative potentials, a single irreversible process is observed. Two consecutive irreversible anodic peaks appear at 0.25 V and 0.35 V vs Ag/AgCl. These processes are due to adsorbed species from CO_2 reduction products. After 50 scans the voltammetric response becomes stable, and the original voltammetric response can be recovered.

The charge of the $Ru^{III/II}$ process for this electrode decreases 2.8% and 31.5% for the anodic and cathodic peak, respectively.

In the case of the $[Zn(II)TRP]^{4+}/[SiW_{12}O_{40}]^{4-}$ multilayer modified electrode, the voltammetric response after the potential controlled electrolysis, shows a charge decrease of 21.5% for the anodic and of 54.8% for the cathodic process of the $Ru^{III/II}$ couple, however, this modified electrode present the same voltammetric shape than before controlled potential electrolysis experiments (not shown). For the $[Ni(II)TRP]^{4+}/[SiW_{12}O_{40}]^{4-}$ a decrease of 27.8% for the anodic and 16.6% for the cathodic $Ru^{III/II}$ process is observed. The voltammetric shape of this multilayer modified electrode also does not exhibit a change compared with the voltammetric response before potential controlled electrolysis experiments.

The difference in the electrocatalytic activity of each multilayer modified electrode can be attributed to the difference on the metal ion center of the porphyrin that can influence the morphological and electrochemical properties. Reported data, confirm [57] that $[Mn(III)TRP]^{5+}/[SiW_{12}O_{40}]^{4-}$ multilayer are thicker (ca. 218 nm) and compact than $[Zn(II)TRP]^{4+}/[SiW_{12}O_{40}]^{4-}$ multilayer (ca.60.3 nm) because the Mn(III) atom interacts strongly with the $[SiW_{12}O_{40}]^{4-}$ anion, giving rise to a more ordered film and thus more coverage of the electrode surface. On the other hand, it has been reported that these porphyrins generate non-homogenous films, giving rise to different microenvironments into the multilayer structure in which active sites can be randomly distributed, giving rise to different electrocatalytic behavior.

$[Zn(II)TRP]^{4+}$ multilayer films produce formic acid and the biggest amount of methanol. This can be explained in terms of the reduction processes of the film. As it can be seen in Fig. 4, this modified electrode shows two reduction waves corresponding to the multilayer reduction, thus at the working potential (−0.8 V vs Ag/AgCl) there will a higher charge density on the electrode surface. Even though Zn^{2+} does not have d orbitals available (closed shell ion) to allow carbon dioxide coordination, there are reports of carbon dioxide reduction catalyzed by imidazolium and pyridinium derivatives [68,69], were the reduction takes place via coordination to the N atom due to its acidic properties [68,69]. A higher charge density in the $[Zn(II)TRP]^{4+}/[SiW_{12}O_{40}]^{4-}$ multilayer film, could allow a reduction via the *N* groups of the porphyrin. This behavior is in strong agreement with the fact that after controlled potential electrolysis experiments, the charge of the electrode decreases over a 50% of the initial value due to film degradation.

3.4. Photoelectrochemical reduction of carbon dioxide

Taking into account that these multilayer modified electrodes display catalytic activity for carbon dioxide reduction, and that these multilayer films present multiple electronic transitions in the range of visible light, the combination of applied potential and light can be of great interest for CO_2 reduction.

Table 3
Potential controlled electrolysis under irradiation of 440 nm results; after 3 h, 0.1 M $NaClO_4$ solutions saturated with CO_2, at −0.65 V.

Multilayer	Formic acid (mM)	TOF (s^{-1})	TON	Methanol (mM)	TOF (s^{-1})	TON	Fornaldehyde (mM)	TOF (s^{-1})	TON
$[Mn(III)TRP]^{5+}/[SiW_{12}O_{40}]^{4-}$	–	–	–	–	–	–	1.8	16.7	1.8×10^5
$[Zn(II)TRP]^{4+}/[SiW_{12}O_{40}]^{4-}$	2.3×10^{-2}	1.3×10^{-1}	1.4×10^3	1.26×10^{-1}	7.3×10^{-1}	7.9×10^3	–	–	
$[Ni(II)TRP]^{5+}/[SiW_{12}O_{40}]^{4-}$	–	–		–	–		5.5×10^{-1}	1.78	3.85×10^4
Bare ITO	1.8×10^{-2}	–		–	–		–	–	

Fig. 6 displays *I/E* curves of $[MTRP]^{n+}/[SiW_{12}O_{40}]^{4-}$ multilayer modified electrodes in pseudo steady state conditions recorded at 5 mV s^{-1} in presence of CO_2 in dark and under irradiation.

The three modified electrodes, present an increase in the current response under irradiation with light at 440 nm. A new reduction peak appears at approximately −0.60 V vs Ag/AgCl for the three multilayer modified electrodes. At −0.65 V vs Ag/AgCl $[Mn(III)TRP]^{5+}/[SiW_{12}O_{40}]^{4-}$ multilayer modified electrode present an increase in the current of 3.2 times compared to its behavior in dark conditions, $[Zn(II)TRP]^{4+}/[SiW_{12}O_{40}]^{4-}$ and $[Ni(II)TRP]^{4+}/[SiW_{12}O_{40}]^{4-}$ multilayer modified electrode present a current increase of 8.2 and 3.3 times respectively compared to dark conditions. The observed current increase is due to carbon dioxide reduction at these multilayer systems. To evaluate the behavior under light irradiation, potential controlled electrolysis experiments were carried out. The potential chosen for this experiment at all electrodes was −0.65 V vs Ag/AgCl. Results obtained for the photoelectrochemical reduction of CO_2 are presented in Table 3.

Under light irradiation, there is a change in the product distribution, with formaldehyde production detected as the major product

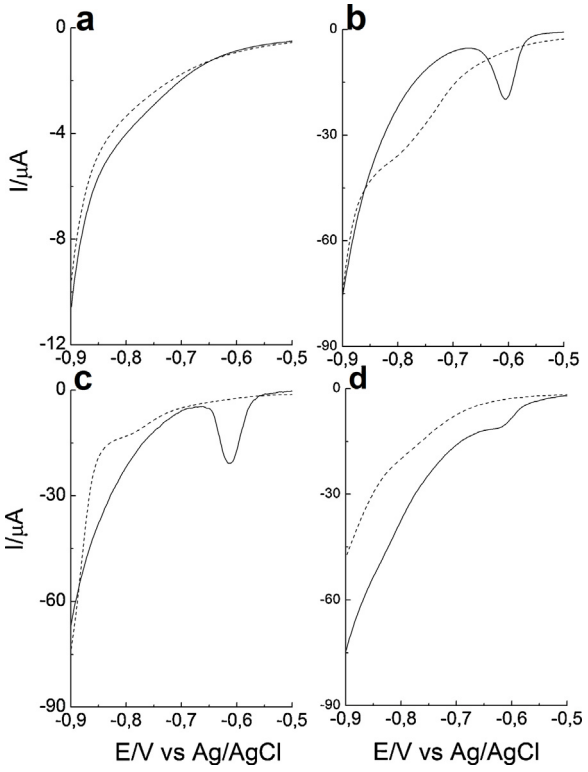

Fig. 6. Linear sweep voltammogram of (a) bare ITO electrode (b) $[Mn(III)TRP]^{5+}/[SiW_{12}O_{40}]^{4-}$ multilayer modified electrode (c) $[Zn(II)TRP]^{4+}/[SiW_{12}O_{40}]^{4-}$ modified electrode and (d) $[Ni(II)TRP]^{4+}/[SiW_{12}O_{40}]^{4-}$ modified electrode in presence of CO_2 in dark (dashed line) and under light irradiation of 440 nm (solid line). 0.1 M $NaClO_4$ solution saturated with CO_2 at 5 mV s^{-1}. Potentials are versus Ag/AgCl.

in electrolysis results. Formaldehyde formation involves the transfer of four electrons as shown in Eq. (4).

$$CO_2 + 4H^+ + 4e^- \rightarrow HCOH + H_2O \quad (4)$$

In the case of $[Mn(III)TRP]^{5+}/[SiW_{12}O_{40}]^{4-}$ multilayer electrode, electrolysis result show the formation of formaldehyde as the only product, rather than formic acid and methanol formation in dark conditions. $[Ni(II)TRP]^{4+}/[SiW_{12}O_{40}]^{4-}$ multilayer modified electrodes present a similar behavior where only formaldehyde formation can be detected. Both results, involve a change in the reduction mechanism of carbon dioxide under light irradiation.

On the other hand, $[Zn(II)TRP]^{4+}/[SiW_{12}O_{40}]^{4-}$ multilayer modified electrode shows a 12 fold increase in the amount of formic acid produced against dark conditions, showing that under light conditions, formic acid production is favored. Despite light and potential combination, methanol production decreases approximately 30 folds. This result together with non-production of methanol with $[Mn(III)TRP]^{5+}/[SiW_{12}O_{40}]^{4-}$ multilayer suggests that, carbon dioxide reduction to methanol on this films depends strongly on the applied potential.

Bare ITO electrode, also shows an increase of approximately 20 folds in the amount of formic acid production.

It is important to mention that for the $[Mn(III)TRP]^{5+}/[SiW_{12}O_{40}]^{4-}$, $[Ni(II)TRP]^{4+}/[SiW_{12}O_{40}]^{4-}$ multilayer modified electrode, and for the bare ITO electrode, the amount of total product obtained under light irradiation is more than that obtained in dark conditions. For the $[Zn(II)TRP]^{4+}/[SiW_{12}O_{40}]^{4-}$ multilayer, despite a decrease in the total amounts of products, the formation of formic acid increases, indicating the electrode becomes selective in these conditions.

All results support the idea of an enhancement in the catalytic activity of the modified electrodes and bare ITO electrode, considering that the potential was 150 mV more positive than in dark conditions and the electrolysis time was halved.

Based on literature reports, TRP films are known to undergo energy transfer processes and that there are strong electronic interactions between both sites of the complex, promoting an energy transfer process from $Ru(bipy)_2Cl^+$ moieties to the porphyrin central core [55]. In such cases, the $Ru(bipy)_2Cl^+$ moieties work as antennae, absorbing light and transferring energy within the film. Several other examples demonstrate that TRP films are photoactive to electrochemical reduction of oxygen [28] or can act as a photo-sensitizer for solar cells [70].

Based on the properties described above, we can conclude that for the films presented in this work, light absorption leads to an improvement in the electronic transfer, promoting

(a) The reduction of carbon dioxide via four electrons, to produce formaldehyde.
(b) An increase in the electron transfer kinetics towards carbon dioxide reduction
(c) An increase in the number of catalytic sites.

Resulting a bigger amount of the same reduction products than in dark conditions.

4. Conclusions

Carbon dioxide reduction was studied in aqueous solution, using a [MTRP]/$[SiW_{12}O_{40}]^{4-}$ multilayer modified electrodes, with M = Mn(III), Ni(II) and Zn(II). The experiments were carried in dark and under light irradiation (440 nm). In dark conditions, the three modified electrodes showed electrocatalytic activity; moreover, carbon monoxide, formic acid and methanol production were detected as the reduction products. The electrocatalytic activity of the films is governed by the metal ion in the center of the porphyrin, which can direct the morphology and electrochemical properties. Due to this, different microenvironments in the multilayer arrangement can be found, which can then produce different reduction products. The $[Zn(II)TRP]^{4+}/[SiW_{12}O_{40}]^{4-}$ multilayer, reduces carbon dioxide obtaining formic acid and methanol in considerable concentration; this effect is due to the electrochemical properties of the film that increase the charge density on the surface.

Under light irradiation, formaldehyde appears as a new product, serving as evidence of a mechanism change for carbon dioxide reduction on $[Mn(III)TRP]^{5+}/[SiW_{12}O_{40}]^{4-}$ and $[Ni(II)TRP]^{4+}/[SiW_{12}O_{40}]^{4-}$ multilayer modified electrode. $[Zn(II)TRP]^{4-}/[SiW_{12}O_{40}]^{4-}$ film, present a change in the proportion of the amount of obtained product. It was clear, that methanol production depends on the applied potential in the experiments.

It was demonstrated that in less favorable conditions (150 mV less negative and half of the time, for controlled potential electrolysis experiments) larger amounts of reduction products were detected. Thus combination of potential and light, give rise to a synergic effect, which increases the reactivity of the film for carbon dioxide reduction. These encouraging results; open a new possibility for studies on the photoelectrochemical properties of these multilayer modified films toward molecules with environmental significance.

Acknowledgment

The authors acknowledge the financial support of FONDECYT, project #1100203 and ICM-P10-003-F, CILIS, granted by Fondo de Innovación para la Competitividad del Ministerio de Economía, Fomento y Turismo, Chile. M.G. acknowledges the CONICYT scholarships for Ph.D. studies in Chile, Ph.D. scholarship support AT 24110089 and the Ph.D. exchange student program (BECAS CHILE) and FULBRIGHT CHILE exchange student program. G.C. and C.P.K. acknowledge support from the NSF CHE-1145893.

Appendix A. Supplementary data

Supplementary data associated with this article can be found, in the online version, at http://dx.doi.org/10.1016/j.electacta.2013.10.142.

References

[1] R. Chaplin, A. Wragg, Effects of process conditions and electrode material on reaction pathways for carbon dioxide electroreduction with particular reference to formate formation, Journal of Applied Electrochemistry 33 (2003) 1107–1123.
[2] M.M. Halman, M. Steinberg, Greenhouse Gas Carbon Dioxide Mitigations Science and Technology, Lewis Publishers, Boca Raton, FL, 1999.
[3] G.-Q. Yuan, H.-F. Jiang, C. Lin, S.-J. Liao, Efficient electrochemical synthesis of 2-arylsuccinic acids from CO_2 and aryl-substituted alkenes with nickel as the cathode, Electrochimica Acta 53 (2008) 2170–2176.
[4] T. Yoshida, K. Kamato, M. Tsukamoto, T. Iida, D. Schlettwein, D. Wöhrle, M. Kaneko, Selective electroacatalysis for CO_2 reduction in the aqueous phase using cobalt phthalocyanine/poly-4-vinylpyridine modified electrodes, Journal of Electroanalytical Chemistry 385 (1995).
[5] C. Wang, X.-X. Ma, J. Li, L. Xu, F. Zhang, Reduction of CO_2 aqueous solution by using photosensitized-TiO_2 nanotube catalysts modified by supramolecular metalloporphyrins-ruthenium(II) polypyridyl complexes, Journal of Molecular Catalysis A: Chemical 363-364 (2012) 108–114.
[6] T. Arai, S. Sato, K. Uemura, T. Morikawa, T. Kajino, T. Motohiro, Photoelectrochemical reduction of CO(2) in water under visible-light irradiation by a p-type InP photocathode modified with an electropolymerized ruthenium complex, Chemical Communications (Cambridge, England). 46 (2010) 6944–6946.
[7] H. Ishida, K. Tanaka, Electrochemical COP reduction catalyzed by [Ru(bpy)2(C0)2]2+ and [Ru(bpy2(CO)Cl]+. the effect of pH on the formation of CO and HCOO–, Organometallics 6 (1987) 181–186.
[8] H. Takeda, O. Ishitani, Development of efficient photocatalytic systems for CO_2 reduction using mononuclear and multinuclear metal complexes based on mechanistic studies, Coordination Chemistry Reviews 254 (2010) 346–354.
[9] E. Portenkirchner, K. Oppelt, C. Ulbricht, D.A.M. Egbe, H. Neugebauer, G. Knör, et al., Electrocatalytic and photocatalytic reduction of carbon dioxide to carbon monoxide using the alkynyl-substituted rhenium(I) complex (5,5′-bisphenylethynyl-2,2′-bipyridyl)Re(CO)3Cl, Journal of Organometallic Chemistry 716 (2012) 19–25.
[10] M. Gattrell, N. Gupta, a. Co, A review of the aqueous electrochemical reduction of CO_2 to hydrocarbons at copper, Journal of Electroanalytical Chemistry 594 (2006) 1–19.
[11] M. Jitaru, D. Lowy, M. Toma, Electrochemical reduction of carbon dioxide on flat metallic cathodes, Journal of Applied Electrochemistry 27 (1997) 875–889.
[12] K.W. Trese, in: B.P. Sullivan, K. Krist, H.E. Guard (Eds.), Electrochemical and electrocatalytic reactions of carbon dioxide, Elsevier B.V., Amsterdam, 1996.
[13] R. Hinogami, Y. Nakamura, An approach to ideal semiconductor electrodes for efficient photoelectrochemical reduction of carbon dioxide by modification with small metal particles, The Journal of Physical Chemistry B 5647 (1998) 974–980.
[14] H. Flaisher, R. Tenne, M. Halmann, Photoelectrochemical reduction of carbon dioxide in aqueous solutions on p-GaP electrodes: an ac impedance study with phase-sensitive detection, Journal of Electroanalytical Chemistry 402 (1996) 97–105.
[15] S. Kaneco, H. Katsumata, T. Suzuki, K. Ohta, Photoelectrochemical reduction of carbon dioxide at p-type gallium arsenide and p-type indium phosphide electrodes in methanol, Chemical Engineering Journal 116 (2006) 227–231.
[16] S. Kaneco, Y. Ueno, H. Katsumata, T. Suzuki, K. Ohta, Photoelectrochemical reduction of CO_2 at p-InP electrode in copper particle-suspended methanol, Chemical Engineering Journal 148 (2009) 57–62.
[17] J. Costamagna, G. Ferraudi, Carbon dioxide activation by aza-macrocyclic complexes, Coordination Chemistry Reviews 148 (1996) 221–248.
[18] S. Chardon-Noblat, P. Da Costa, Electrosynthesis, physico-chemical and electrocatalytic properties of a novel electroactive Ru(0) material based on the (Ru(terpy)(CO)) frame (terpy = 2, 2′: 6′, 2′′-terpyridine, Journal of Electroanalytical Chemistry 529 (2002) 135–144.
[19] J.R. Sende, C. Arana, L. Hernández, K.T. Potts, M.K. Kesevarz, H.D. Abruña, Electrocatalysis of CO_2 reduction in aqueous media at electrodes modified with electropolymerized films of vinylterpyridine complexes of transition metals, Inorganic Chemistry 34 (1995) 3339–3348.
[20] F. Cecchet, M. Alebbi, C.A. Bignozzi, F. Paolucci, Efficiency enhancement of the electrocatalytic reduction of CO_2: fac-[Re(v-bpy)(CO)3Cl] electropolymerized onto mesoporous TiO_2 electrodes, Inorganica Chimica Acta 359 (2006) 3871–3874.
[21] M. Isaacs, F. Armijo, G. Ramírez, E. Trollund, S.R. Biaggio, J. Costamagna, M.J. Aguirre, Electrochemical reduction of CO_2 mediated by poly-M-aminophthalocyanines (M = Co, Ni, Fe): poly-Co-tetraaminophthalocyanine, a selective catalyst, Journal of Molecular Catalysis A: Chemical 229 (2005) 249–257.
[22] M.A. Riquelme, M. Isaacs, M. Lucero, E. Trollund, M.J. Aguirre, Electrocatalytic reduction of carbon dioxide at polymeric cobalt tetra(3-amino (phenyl)) porphyrin glassy carbon modified electrodes, Journal of the Chilean Chemical Society 48 (2003) 89.
[23] E. Simón-Manso, C. Kubiak, Dinuclear nickel complexes as catalysts for electrochemical reduction of carbon dioxide, Organometallics 24 (2005) 96–102.
[24] R. Schrebler, P. Cury, C. Sua, E. Mun, R. Co, Study of the electrochemical reduction of CO_2 on a polypyrrole electrode modified by rhenium and copper rhenium microalloy in methanol media, Journal of Electroanalytical Chemistry 533 (2002) 167–175.
[25] J.L. Inglis, B.J. MacLean, M.T. Pryce, J.G. Vos, Electrocatalytic pathways towards sustainable fuel production from water and CO_2, Coordination Chemistry Reviews 256 (2012) 2571–2600.
[26] H. Zhao, Y. Zhang, B. Zhao, Y. Chang, Z. Li, J.L. Inglis, et al., Electrochemical reduction of carbon dioxide in an MFC–MEC system with a layer-by-layer self-assembly carbon nanotube/cobalt phthalocyanine modified electrode, Environmental Science & Technology 46 (2012) 5198–5204.
[27] K. Araki, H.E. Toma, Synthesis and characterization of a multibridged porphyrin complex containing peripheral bis(bipyridine)-ruthenium(II) groups, Jounal of Coordination Chemistry 30 (1993) 9–17.
[28] K. Araki, M. Wagner, M. Wrighton, Layer-by-layer growth of electrostatically assembled multilayer porphyrin films, Langmuir 7463 (1996) 5393–5398.
[29] K. Calfumán, M.J. Aguirre, D. Villagra, C. Yañez, C. Arévalo, B. Matsuhiro, L. Mendoza, M. Isaacs, Nafion/tetraruthenated porphyrin glassy carbon-modified electrode: characterization and voltammetric studies of sulfite oxidation in water–ethanol solutions, Journal of Solid State Electrochemistry 14 (2010) 1065–1072.

[30] H.E. Toma, K. Araki, Supramolecular assemblies of ruthenium complexes and porphyrins, Coordination Chemistry Reviews 196 (2000) 307–329.
[31] I. Mayer, M. Nakamura, H.E. Toma, K. Araki, Multielectronic redox and electrocatalytic supramolecular films based on a tetraruthenated iron porphyrin, Electrochimica Acta 52 (2006) 263–271.
[32] I. Mayer, H.E. Toma, K. Araki, Electrocatalysis on tetraruthenated nickel and cobalt porphyrins electrostatic assembled films, Journal of Electroanalytical Chemistry 590 (2006) 111–119.
[33] H. Ishida, T. Terada, K. Tanaka, T. Tanaka, Photochemical COz reduction catalyzed by [Ru(bpy)2(C0)2]2+ using triethanolamine and 1-benzyl-1,4-dihydronicotinamide as an electron donor, Inorganic Chemistry 29 (1990) 905–911.
[34] A. Tinnemans, Tetraaza-macrocyclic cobalt(II) and nickel(II) complexes as electron-transfer agents in the photo(electro) chemical and electrochemical reduction of carbon dioxide, Journal of the Royal Netherlands Chemical Society 103 (1984) 288–295.
[35] K. Mochizuki, S. Manaka, I. Takeda, T. Kondo, Synthesis and structure of activity for photochemical CO_2 reduction, Inorganic Chemistry 35 (1996) 5132–5136.
[36] J. Grant, K. Goswami, L. Spreer, Photochemical reduction of carbon dioxide to carbon monoxide in water using a nickel(II) tetra-azamacrocycle complex as catalyst, Journal of the Chemical Dalton Transaction (1987) 2105–2109.
[37] B. Kumar, J. Smieja, C. Kubiak, Photoreduction of CO_2 on p-type silicon using Re(bipy-Bu t)(CO)3Cl: photovoltages exceeding 600 mV for the selective reduction of CO_2 to CO, The Journal of Physical Chemistry C 114 (2010) 14220–14223.
[38] D.-L. Long, E. Burkholder, L. Cronin, Polyoxometalate clusters, nanostructures and materials: from self assembly to designer materials and devices, Chemical Society Reviews 36 (2007) 105–121.
[39] D. Ingersoll, P.J. Kulesza, L.R. Faulkner, Polyoxometallate based layered composite films on electrodes: preparation through alternate immersions in modification solutions, Journal of The Electrochemical Society 141 (1994) 140–147.
[40] H. Ma, Z. Zhang, H. Pang, S. Li, Y. Chen, W. Zhang, Fabrication and electrochemical sensing property of a composite film based on a polyoxometalate and palladium nanoparticles, Electrochimica Acta 69 (2012) 379–383.
[41] J. Xin, T. Lindenmuth, C. Shannon, Electrocatalytic oxygen reduction at polyoxometalate/Au-nanoparticle hybrid thin films formed by layer-by-layer deposition, Electrochimica Acta 56 (2011) 8884–8890.
[42] S. Zoladek, I.A. Rutkowska, K. Skorupska, B. Palys, P.J. Kulesza, Fabrication of polyoxometallate-modified gold nanoparticles and their utilization as supports for dispersed platinum in electrocatalysis, Electrochimica Acta 56 (2011) 10744–10750.
[43] D.M. Fernandes, M.E. Ghica, A.M.V. Cavaleiro, C.M.A. Brett, Electrochemical impedance study of self-assembled layer-by-layer iron–silicotungstate/poly(ethylenimine) modified electrodes, Electrochimica Acta 56 (2011) 7940–7945.
[44] P.J. Kulesza, M. Chojak, K. Miecznikowski, A. Lewera, M.A. Malik, A. Kuhn, Polyoxometallates as inorganic templates for monolayers and multilayers of ultrathin polyaniline, Electrochemistry Communications 4 (2002) 510–515.
[45] R. Sivakumar, J. Thomas, M. Yoon, Polyoxometalate-based molecular/nano composites: advances in environmental remediation by photocatalysis and biomimetic approaches to solar energy, Journal of Photochemistry and Photobiology C: Photochemistry Reviews 13 (2012) 277–298.
[46] Y. Shen, J. Liu, J. Jiang, B. Liu, S. Dong, Fabrication of a metalloporphyrin-polyoxometalate hybrid film by a layer-by-layer method and its catalysis for hydrogen evolution and dioxygen reduction, The Journal of Physical Chemistry B 107 (2003) 9744–9748.
[47] S. Dong, X. Xi, M. Tian, Study of the electrocatalytic reduction of nitrite with silicotungstic heteropolyanion, Journal of Electroanalytical Chemistry 385 (1995) 227–233.
[48] K.M. Wiaderek, A.J. Cox, Preparation and electrocatalytic application of composites containing gold nanoparticles protected with rhodium-substituted polyoxometalates, Electrochimica Acta 56 (2011) 3537–3542.
[49] D.M. Fernandes, C.M.A. Brett, A.M.V. Cavaleiro, Layer-by-layer self-assembly and electrocatalytic properties of poly(ethylenimine)-silicotungstate multilayer composite films, Journal of Solid State Electrochemistry 15 (2010) 811–819.
[50] G. Bazzan, W. Smith, L.C. Francesconi, C.M. Drain, Electrostatic self-organization of robust porphyrin-polyoxometalate films, Langmuir: The ACS Journal of Surfaces and Colloids 24 (2008) 3244–3249.
[51] Y. Shen, J. Liu, J. Jiang, B. Liu, S. Dong, Fabrication of metalloporphyrin-polyoxometalyte hybrid film by layer-by-layer method and its catalysis for dioxygen reduction, Electroanalysis 14 (2002) 1557–1563.
[52] D. Martel, M. Gross, Electrochemical study of multilayer films built on glassy carbon electrode with polyoxometalate anions and two multi-charged molecular cationic species, Journal of Solid State Electrochemistry 11 (2006) 421–429.
[53] S.P. Sullivan, D.J. Salmon, T. Meyer, Mixed phosphine 2,2′-bipirydine complexes of ruthenium, Inorganic Chemistry 17 (1978) 3334–3341.
[54] K. Araki, L. Angnes, H.E. Toma, Rectifying properties and photoconductivity of tetraruthenated nickel porphyrin films, Advanced Materials 7 (1995) 554–559.
[55] K. Araki, H.E. Toma, Luminescence, spectroelectrochemistry and photoelectrochemical properties of a tetraruthenated zinc porphyrin, Journal of Photochemistry and Photobiology A: Chemistry 83 (1994) 245–250.
[56] C.M.N. Azevedo, K. Araki, L. Angnes, H.E. Toma, Electrostatically assembled films for improving the properties of tetraruthenated porphyrin modified electrodes, Electroanalysis 10 (1998) 467–471.
[57] M. García, K. Calfumán, C. Díaz, C. Garrido, I. Osorio-Román, M.J. Aguirre, M. Isaacs, Multimetallic porphyrins/polyoxotungstate modified electrodes by layer-by-layer method: Electrochemical, spectroscopic and morphological characterization, Electrochimica Acta 80 (2012) 390–398.
[58] P. Paul, B. Tyagi, A.K. Bilakhiya, M.M. Bhadbhade, Synthesis and characterization of rhodium complexes containing uses of the new complexes in electrocatalytic reduction of carbon dioxide, Inorganic Chemistry 37 (1998) 5733–5742.
[59] K. Araki, H. Toma, N4-Macrocyclic Metal Complexes: Supramolecular Porphyrins As Electrocatalysts, New York, NY, 2006.
[60] N. Maiti, J- and H-aggregates of porphyrin–surfactant complexes: time-resolved fluorescence and other spectroscopic studies, The Journal of Physical Chemistry B 5647 (1998) 1528–1538.
[61] P. Kuba, K. Lang, K. Procha, P. Anzenbacher, J. Heyrovsky, Self-aggregates of cationic meso-tetratolylporphyrins in aqueous solutions, Langmuir (2003) 422–428.
[62] S. Verma, A. Ghosh, A. Das, H.N. Ghosh, Ultrafast exciton dynamics of J- and H-aggregates of the porphyrin-catechol in aqueous solution, The Journal of Physical Chemistry. B 114 (2010) 8327–8334.
[63] K. Araki, H. Winnischofer, H.E.B. Viana, M.M. Toyama, F.M. Engelmann, I. Mayer, et al., Enhanced electrochemical and electrocatalytic activity of a new supramolecular manganese-porphyrin species containing four bis(bipyridine)(aqua)ruthenium(II) complexes, Journal of Electroanalytical Chemistry 562 (2004) 145–152.
[64] M. Sadakane, E. Steckhan, Electrochemical properties of polyoxometalates as electrocatalysts, Chemical Reviews 98 (1998) 219–238.
[65] P. Dreyse, M. Isaacs, K. Calfumán, C. Cáceres, A. Aliaga, M.J. Aguirre, D. Villagra, Electrochemical reduction of nitrite at poly-[Ru(5-NO_2-phen)2Cl] tetrapyridylporphyrin glassy carbon modified electrode, Electrochimica Acta 56 (2011) 5230–5237.
[66] Y. Hayashi, N. Komiya, K. Suzuki, S.-I. Murahashi, Copper-catalyzed aerobic oxidative functionalization of C–H bonds of alkanes in the presence of acetaldehyde under mild conditions, Tetrahedron Letters 54 (2013) 2706–2709.
[67] D.K. Dutta, J.D. Woollins, A.M.Z. Slawin, A.L. Fuller, B. Deb, P.P. Sarmah, et al., Rhodium(I) carbonyl complexes of chalcogen functionalized tripodal phosphines, [$CH_3C(CH_2P(X)Ph_2)3$] {X = O, S, Se} and their reactivity, Journal of Molecular Catalysis A: Chemical 313 (2009) 100–106.
[68] A. Bocarsly, Q. Gibson, Comparative study of imidazole and pyridine catalyzed reduction of carbon dioxide at illuminated iron pyrite electrodes, ACS Catalysis 2 (2012) 1684–1692.
[69] E.B. Cole, P.S. Lakkaraju, D.M. Rampulla, A. Morris, E. Abelev, A. Bocarsly, Using a one-electron shuttle for the multielectron reduction of CO_2 to methanol: kinetic, mechanistic, and structural insights, Journal of the American Chemical Society (2010) 11539–11551.
[70] H. Winnischofer, A.L.B. Formiga, M. Nakamura, H.E. Toma, K. Araki, A.F. Nogueira, Conduction and photoelectrochemical properties of monomeric and electropolymerized tetraruthenated porphyrin films, Photochemical & Photobiological Sciences 4 (2005) 359–366.